Supplementary Materials for

Notch-Jagged complex structure implicates a catch bond in tuning ligand sensitivity

Vincent C. Luca, Byoung Choul Kim, Chenghao Ge, Shinako Kakuda, Di Wu, Mehdi Roein-Peikar, Robert S. Haltiwanger, Cheng Zhu, Taekjip Ha, K. Christopher Garcia

Correspondence to: kcgarcia@stanford.edu

This PDF file includes:

MATERIALS AND METHODS:

Protein expression and purification

Fc-tagged rat Jag1 (N-EGF3, amino acids 32-334) was cloned into the pAcGp67A vector with an N-terminal gp67 leader followed by residues Asp-Pro, and contains a C-terminal 3C-protease site followed by IgG1 Fc and 6xHis tags. Fc-tagged rat $Jag1_{JV1}$ (N-EGF3, amino acids 32-334) was cloned into the pAcGp67A vector with an N-terminal gp67 leader sequence followed by residues Asp-Pro-Arg, and contains a C-terminal 3C-protease site followed by IgG1 Fc and 6xHis tags. His-tagged $Jag1_{JV1}$ (N-EGF3, amino acids 32-334) was cloned into the pAcGp67A vector with an N-terminal gp67 leader followed by residues Asp-Pro-Arg, and contains a C-terminal 8xHis tag. His-tagged rat DLL4 (N-EGF3, amino acids 26-321) was cloned into the pAcGp67A vector with an N-terminal gp67 leader followed by residues Gly-Ser, and a C-terminal 8xHis tag. Jag1(N-3), $Jag1_{JV1}$(N-3) and DLL4(N-3) constructs with C-terminal biotin acceptor peptide tags (BAP-tag: GLNDIFEAQKIEW) and 6xHis tags, which were used in BFP experiments, were cloned into pAcGp67A as described above. Rat Notch1 (EGF1-14, amino acids 20-564) was cloned into pAcGp67A with an N-terminal gp67 leader followed by residues Asp-Pro, and with a C-terminal BAP tag and a 6xHis tag. Rat Notch1 (EGF11-12, amino acids 412-488) and Notch1 (EGF8-12, amino acids 295-488) were cloned into pAcGp67A an N-terminal gp67 leader followed by residues Asp-Pro, and contains a C-terminal 3C protease site followed by BAP and 6xHis tags.

All proteins were expressed using baculovirus by infecting Hi-Five cells (Invitrogen) from *Trichoplusia ni* at a density of $2x10^6$ cells/mL and harvesting cultures after 72 hours. Proteins were purified from supernatants by nickel chromatography. Nickel nitrilotriacetic acid agarose resin (Nickel-NTA, Qiagen) was washed with HEPES buffered saline (HBS: 20 mM HEPES pH 7.4, 150 mM sodium chloride) containing 10 mM imidazole, and protein was eluted with HBS containing 250 mM imidazole. Size-exclusion chromatography was performed in HBS on a Superdex-200 column. BAP-tagged Notch1 proteins and ligands used in binding experiments were site-specifically biotinylated at the C-terminal BAP tag with BirA ligase prior to buffer exchange on a size-exclusion column.

Yeast display of Jag1

Wild-type rat Jag1 (N-EGF3, amino acids 32-334) was cloned into the pCT302 vector as an N-terminal fusion to a c-Myc epitope and cell wall protein Aga2. Jag1(N-EGF3) was displayed on *S. cerevisiae* EBY100 yeast as previously reported(*31*). In brief, competent yeast were electroporated with plasmids and recovered in SDCAA selection media. Yeast cultures in logarithmic growth phase were then pelleted and resuspended in SGCAA induction media. Expression of Jag1 was detected by staining yeast with a 488-labeled anti-c-Myc antibody (Cell Signaling), and fluorescence was monitored by flow cytometry.

Jag1 mutant library generation

A mutant library of Jag1(N-3) was generated by PCR amplification of the Jag1(N-3) sequence using the error-prone polymerase from the Genemorph II Kit (Agilent). Various

concentrations of the Jag1(N-EGF3) pCT302 plasmid were used as a template for PCR reactions and sequenced to identify products with an average error rate of ~5 mutations/gene. PCR reactions were then amplified using primers flanking the Jag1 gene that contained homology to the pCT302 vector:

5' T7 forward primer (5' TAATACGACTCACTATAGGG 3')
3' Aga2 reverse primer (5' GGGATTTGCTCGCATATAGTTG 3').

Gel-purified PCR products were combined with linearized pCT302 vector DNA and the mixture was electroporated into EBY100 yeast to obtain a library containing $2x10^8$ transformants. Electroporated yeast were recovered and induced as described above. Prior to the first round of selection, $1x10^9$ yeast from the library were pelleted and resuspended in buffer "HB+CM" (20 mM HEPES pH 7.4, 150 mM NaCl, 1 mM calcium chloride, 10 mM maltose, 0.5% bovine serum albumin (BSA)). Maltose was included in buffers to prevent calcium-mediated flocculation of yeast.

Affinity maturation of Jag1 and fluorescence based binding assays of yeast displayed Jag1 variants

To negatively select against non-specific binders to streptavidin, $1x10^9$ yeast from the Jag1(N-3) library were mixed with 100 μL SA-coated magnetic microbeads (Militenyi) and incubated for 30 minutes, washed with HB+CM and then flowed over a Magnetic-Activated cell sorting (MACS) LS separation column (Militenyi). Round 1 of selection was performed on yeast that flowed through the LS column during negative selection. To perform the round 1 selection, Notch1-coated beads were prepared by diluting biotinylated Notch1(1-14) to a final concentration of 400 nM in a 250 μL aliquot of streptavidin microbeads. The beads were then mixed with the negatively selected yeast in 5 mL HB+CM. Yeast were rocked at 4°C for 2 hours, washed with HB+CM and passed over a MACS column to isolate binders. The enriched yeast were recovered in SDCAA for 24 hours, induced in SGCAA, and the selection process was repeated with $1x10^8$ yeast for round 2. Round 3 was performed by staining $5x10^7$ enriched yeast in 0.5 mL HB+CM with a 100 nM concentration of soluble Notch1(1-14) tetramers. Tetramers were generated by mixing biotinylated Notch1(1-14) at a 4.5 to 1 ratio with streptavidin labeled with Alexafluor-647 dye (SA-647, Life Technologies). Tetramer-stained yeast were rocked at 4°C for 2 hours, washed with HB+CM and then incubated for 20 minutes with 50 μL anti-647 microbeads (Militenyi) in 0.5 mL HB+CM. Yeast were washed with HB+CM and binders were again isolated by MACS. Round 4 was performed as round 3 except yeast were stained with a 25 nM concentration of Notch1(1-14) tetramers. To isolate high-affinity clones, yeast cultures from Round 4 were plated on SDCAA agarose plates and the individual colonies were grown in SDCAA media. Each clone was induced and then screened for binding to Notch1(1-14) tetramers by flow cytometry. Plasmids from high-affinity binders were isolated using the Zymoprep Yeast Plasmid Miniprep II Kit (Zymo Research) and sequenced to identify affinity-enhancing mutations.

To monitor the binding of Jag1-displaying yeast to Notch1, yeast expressing either Jag1(N-3) or $Jag1_{JV1}$(N-3) were induced as described above and then washed with HB+CM. The yeast were then resuspended in 50 μL volumes of HB+CM containing

100 nM concentrations of 647-labeled Notch1(8-12) tetramers and a PE-labeled antibody to the c-Myc epitope (1:100). Samples were incubated at 4°C for 2 hours, washed with HB+CM and then analyzed by flow cytometry. Cell-based assays comparing the binding of $Jag1_{JV1}$(N-3) and $Jag1_{JV1}$ reversion mutants (L32S, G68R, N72D, R87T and Q182R) were performed as described above, except that cells were stained with a series of concentrations of Notch1(8-12) tetramers and performed in triplicate. Mean fluorescence values were then normalized for expression based on c-Myc epitope staining and curves were fitted using Prism 7 (Graphpad) to determine EC50 values. All reversion mutants were generated using PCR and the isothermal assembly cloning method.

SPR binding studies

Dissociation constants of His-tagged rat $Jag1_{JV1}$(N-3) and His-tagged rat DLL4(N-EGF3) for rat Notch1(8-12) and Notch1(11-12) were determined by surface plasmon resonance using a BIAcore T100 instrument (GE Healthcare). Approximately 400 resonance units (RU) of either biotinylated, recombinant Notch1(8-12) or ~400 RU of Notch1(11-12) were immobilized on a streptavidin coated sensor chip (GE Healthcare). Increasing concentrations of recombinant His-tagged Jag1(N-3), $Jag1_{JV1}$(N-3) or DLL4(N-3) proteins were flowed over the chip in HBS supplemented with 0.005% surfactant P20 (HBS+P) containing 1 mM calcium chloride at 20°C. Binding and dissociation phases were performed at 50 µl/min for 60 seconds and 120 seconds, respectively. The chip was regenerated after each injection with 60-second washes of 0.5 M $MgCl_2$. Curves were reference-subtracted from a flow cell containing ~400 RU of a negative control protein (extracellular domain of human ZNRF3). The maximum RU for each experiment was normalized to a value of 100 and plotted as a function of concentration using Prism 6 (GraphPad). Steady-state binding curves were fitted using the BIAcore T100 evaluation software to a 1:1 Langmuir model to determine the K_d. Although binding was observed at high concentrations for WT Jag1(N-3), the curves could not be reliably fitted to obtain K_d values.

Proteolytic processing, deglycosylation and methylation of Notch1 and Jag1

The methods for post-purification processing of Notch1 and Jag1 are adapted from Luca *et al.*(*20*). Notch1(8-12) and His-tagged $Jag1_{JV1}$(N-3) constructs intended for co-crystallization were purified individually, as described above, and then enzymatically treated to remove C-terminal tags and N-linked glycans. $Jag1_{JV1}$(N-3) proteins were expressed in cultures supplemented with 5µM kifunensine at the time of infection. Kifunensine-sensitized $Jag1_{JV1}$(N-EGF3) was purified by nickel and size-exclusion chromatography and then treated at 4° C overnight with 1:500(w/w) Endoglycosidase F1 to remove N-linked glycans and 1:100(w/w) bovine carboxypeptidase A (Sigma) to remove the C-terminal 8xHis tag. The BAP-6xHis tag of Notch1(8-12) was cleaved with 1:100 (w/w) 3C protease and carboxypeptidase A at 4° C overnight. The enzymatically processed Notch1(8-12) and $Jag1_{JV1}$(N-EGF3) proteins were then mixed at a ratio of 1:1. The complex was then reductively methylated prior to crystallization by adding 20µL/mL dimethylamine borane complex (DMAB) (Sigma) and 40 µL/mL 1 M paraformaldehyde (Sigma) (*32*). The solution was incubated for 2-hours on ice, and then this step was repeated a second time prior to a final addition of 10 µL/mL DMAB. The reaction was allowed to proceed overnight at 4°C and was quenched the next day by adding Tris pH

8.0 to a concentration of 0.1 M. Methylated complexes were then purified by size-exclusion chromatography in HBS + 1 mM calcium chloride. Because complexes did not co-elute as a single peak, fractions containing either protein were harvested and pooled.

Crystallization of Notch1(8-12)-Jag1$_{JV1}$(N-3) complex

The proteolytically processed, deglycosylated and methylated Notch1(8-12)-Jag1$_{JV1}$(N-EGF3) complexes were concentrated to ~30 mg/mL in HBS + 1 mM $CaCl_2$ and crystallized by vapor diffusion. Drops containing 0.1 μL of protein were combined with 0.1 μL of mother liquor consisting of 22.5% polyethylene glycol (PEG) 1000, 0.1 M MES pH 6.6 and 3% dextran sulfate M_r (5000) using a Mosquito® liquid handling robot (TTP Labtech). Cryoprotection of the crystals was achieved by transferring them to a drop containing 22.5% PEG1000, 0.1 M MES pH 6.6, 3% dextran sulfate M_r(5000) and 30% ethylene glycol.

Data collection and structure determination

The data were collected at Advanced Photon Source beamline 23-ID-B. Data were indexed, integrated, scaled and merged with the HKL2000 package(*33*). Notch1(8-12) and Jag1$_{JV1}$(N-EGF3) crystallized in space group $I2_12_12_1$ with unit cell dimensions a = 68.5, Å b = 128.0 Å, c = 154.3 Å, and one complex per asymmetric unit. The structure of the Notch1(8-12)-Jag1$_{JV1}$(N-3) complex was solved using molecular replacement (MR). Models for the individual domains of Jag1$_{JV1}$(N-EGF3) were obtained from the previously solved structure of Jag1(N-3) (PDB ID 4CC0), models for Notch1 EGF domains 11-12 were obtained from the structure of the Notch1-DLL4 complex (PDB ID 4XL1), and a threaded model for Notch1 EGF domain 8 was generated using Phyre2(*17*, *20*, *34*). The MR was performed in PHENIX using Phaser (*35*, *36*). Following placement of the Jag1 C2, DSL and EGF domains 1 through 3, and the Notch1 EGF domains 8, 11 and 12, there was sufficient phase information to allow for manual building of Notch1 EGF domains 9 and 10. Models were initially subjected to rigid body refinement, and then were subjected to several rounds of positional, occupancy, TLS and B-factor refinement using PHENIX Refine, and manual building was performed in Coot (*37–39*). The final structure has an R_{work} of 21.9% and R_{free} of 26.3% and contained Jag1$_{JV1}$ residues 32 to 334 and Notch1 residues 298 to 488.

Structural analysis of Notch1-Jag1$_{JV1}$ complex

Mean buried surface areas were calculated using the PDBe-PISA web server(*40*). Contact residues, hydrogen bonds and salt bridges were identified using PDBe-PISA, Pymol and by manual inspection. Figures were generated in Pymol(*41*). Relative differences in the angles between unliganded Jag1(N-3) (PDB ID 4CC0) and Jag1$_{JV1}$(N-3) domains were determined by aligning individual domains and analyzing the structures with Dyndom(*42*).

Mutagenesis of O-fucosylation sites on EGF8 and EGF12 in Notch1

Site-directed mutagenesis of *O*-fucosylation sites in EGF repeats of in the pcDNA1-Notch1-Myc plasmid was performed using the QuikChange II XL site-Directed Mutagenesis Kit (Agilent Technologies) according to the manufacturer's protocol. Mutations were designed to eliminate the modified residue (threonine to valine) within

the *O*-fucosylation consensus sequence, $C^2xxxx(\underline{S/T})C^3$. The mutants were confirmed via DNA sequencing.

Primers for mutagenesis are provided below:

EGF repeat	
EGF08_T311V_F	gccagaatggcggaGTctgccacaacac
EGF08_T311V_R	gtgttgtggcagACtccgccattctggc
EGF12_T466V_F	gtcagaatgatgccGTttgcctggaccagattgg
EGF12_T466V_R	ccaatctggtccaggcaaACggcatcattctgac

Cell-based Notch1-Jag1 binding assay

HEK293T cells (8.5×10^5) were co-transfected with either EV or pcDNA-Notch1-Myc (WT or mutant) and 0.4 μg of GFP (pEGFP, Clontech) in a 3.5-cm plate using Lipofectamine 2000 (Invitrogen) according to the manufacturer's instructions. At 28-30 h posttransfection, the cells were dissociated with cold PBS, pH 7.4, containing 1% bovine serum albumin (BSA) and resuspended in binding buffer (1 mM $CaCl_2$, 1% BSA and 0.05% NaN_3 in Hank's balanced salt solution, pH 7.4, Gibco). Cells ($0.5\text{-}1.0 \times 10^6$) were incubated with 100 μl of Jag1-Fc (2.1nM, R&D systems) that had been pre-incubated with secondary antibodies (PE-anti human IgG, 1:100, Jackson Immuno Research) for 30 min at 4°C to cluster ligands. The clustered ligands were incubated with Notch1-expressing cells for 1 h at 4°C. Cells were then washed with binding buffer and analyzed with a FACSCalibur (BD, Bioscience) flow cytometer. Cells were gated to collect the GFP positive population for each sample and the data were analyzed using FlowJo®.

To monitor surface expression of Notch1 and Notch1 mutants, co-transfected HEK293T cells were dissociated and resuspended in the binding buffer as described above, followed by incubation with 100 μl of a sheep antibody to mouse Notch-1 (10 μg/ml, R&D Systems AF5267) for 1 h at 4°C. Cells were then washed with binding buffer and incubated with PE-anti-sheep IgG (1:100, Santa Cruz SC-3757) for 30 min at 4°C. Cells were next washed with binding buffer and analyzed as described above.

Cell-based co-culture Notch1 activation assay

HEK293T cells (0.3×10^5) were seeded in a 48-well tissue culture plate and co-transfected 0.05 μg of empty vector, wild type or mutant pcDNA1-mNotch1-Myc plasmid, along with 0.05 μg of TP1-1 luciferase reporter construct and 0.025 μg of gWIZ β-galactosidase construct for transfection efficiency normalization, using 1 μl of PEI (polyethylenimine) well as transfection reagent. After 4 h, either L cells or L cells stably expressing of J1 were overlaid on the transfected 293T cells at a density of 2×10^5 cell/well. After 24h of co-culture, cells were lysed and luciferase assays were performed based on the manufacturer's instructions (Luciferase Assay system, Promega) as described previously (*21*, *43*). Relative Luciferase Units (RLU) were determined by dividing normalized luciferase values from Jag1-expressing cells by that from L cells. Statistical significance of WT Notch1 versus each mutant was determined using one-way ANOVA. Bar graphs in Fig. 2B show mean +/- SD; two independent experiments n = 6 were analyzed.

Biomembrane force probe (BFP) measurement of Notch-ligand bond lifetimes

BFP preparation

In our BFP setup, a biotinylated RBC was first aspirated by a micropipette. A glass bead, coated with streptavidin that had been mutated to contain only one biotin binding site, was incubated with biotinylated Jag1(N-3), $Jag1_{JV1}$(N-3) or DLL4(N-3). The bead was then attached to the apex of the RBC to form an ultra-sensitive force probe. On the opposite side, a similar streptavidin bead, coated with biotinylated Notch1(8-12), was aspirated by a target micropipette. Beads coated with Notch1(8-12) were treated with soluble biotin at 10 μg/ml to block the remaining streptavidin on the beads, and to prevent non-specific interaction. A piezoelectric translator (Physical Instrument, MA) drove the target pipette with sub-nanometer precision via a capacitive sensor feedback control. The beads were assembled in a cell chamber filled with L15 media supplemented with 5 mM HEPES and 1% BSA and observed under an inverted microscope (Nikon TiE, Nikon) through two cameras. One camera (GC1290, Prosilica, MA) captured real-time images at 30 frames per second (fps), while the other (GE680, Prosilica, MA), which recorded at 1,600 fps, was confined to the contact interface between the RBC and the bead as the region of interest. A customized LabView (National Instrument, TX) program analyzed the image and tracked the position of the bead in real-time with a 3 nm displacement precision (*44*). The BFP spring constant was set to ~0.3 pN/nm, which was determined from the suction pressure inside the probe pipette that held the RBC, the inner radius of the probe pipette, the diameter of the spherical portion of the RBC outside of the pipette, and the contact area between the RBC and the probe bead (*44*, *45*).

Lifetime measurement using force-clamp

In one measurement cycle, a Notch1(8-12)-coated bead on a target pipette was brought into contact with the probe bead coated with Jag1(N-3), $Jag1_{JV1}$(N-3) or DLL4(N-3) with a 20 pN impingement force for 1 s to allow bond formation. The target pipette was then retracted at 1000 pN/s and held at the desired force level to wait for bond dissociation. Lifetime was measured as the amount of time the bond was sustained at that particular force level. Following bond dissociation, the target bead was returned to the original position to start the next cycle. To ensure that most adhesion events were contributed by single bonds, adhesion frequency (number of adhesions divided by total number of contacts) was controlled to be ≤20% by adjusting the coating density of proteins on the beads(*46*).

Thermal fluctuation assay

Thermal fluctuation assays measure protein-protein interaction in the absence of force. Similar to the force-clamp assay, the bead coated with Notch1(8-12) was brought into contact with the bead coated with Jag1(N-3), $Jag1_{JV1}$(N-3) or DLL4(N-3), but retraction after contact stopped at the point where impingement force was no longer present. The association and dissociation of protein-protein interactions can be identified from the reduction and resumption of thermal fluctuation derived from the standard deviation of the signal. Combined with the force-clamp assay, bond lifetimes were measured at a force range between 0 pN and 25 pN, and all the measured lifetimes were binned into

different force groups and represented as average lifetime in each force bin associated with the standard error of the mean of the lifetimes in that bin.

Tension gauge tether assay for Notch activation

Ligand-ProG-TGT synthesis

To determine the molecular tension requirements for Notch activation by Fc-tagged Jag1(N-3), Jag1$_{JV1}$(N-3) and DLL4(N-3) ligands, we generated tension gauge tether (TGT) surfaces adapted for Protein G (ProG)-mediated capture of ligands via their Fc tag. ProG-TGT was fabricated as described in detail in Wang *et al.*(*47*). Protein G was conjugated to the 3' end of 18 nucleotide ssDNA (5-/5Cy3/GGC CCG CAG CGA CCA CCC/3ThioMC3-D/3) via a hetero-bifunctional cross-linker (Sulfo-SMCC, Thermo Fisher Scientific Inc.). Sulfo-SMCC has maleimide and NHS ester groups on two ends which react with the –SH group on the –SH modified ssDNA, and with amines on ProG. Complementary ssDNA with a biotin determining the rupture force tolerance (either 12 or 54 pN) were then hybridized to form ProG-TGT. Next, Jag1(N-3), Jag1$_{JV1}$(N-3) or DLL4(N-3) were bound to the ProG-conjugated TGT, resulting in ligand-ProG-TGT (12 or 54 pN). The 4 pN tether was constructed slightly differently, as described in Chowdhury *et al.*(*5*). Briefly, the 4 pN tether was generated by first hybridizing the 18 nt ssDNA-ProG and a long complementary strand, with extra dTs instead of biotin, (5-/AGG TCG CCG CCC GGG TGG TCG CTG CGG GCC TTT TTT TTT TTT TTT TTT TTT TTT TTT TTT TTT TTT TTT TTT TTT TTT TTT TTT TTT TTT TT/3) in PBS buffer overnight at 4° C. Jag1(N-3), Jag1$_{JV1}$(N-3) or DLL4(N-3) were bound to the ProG-conjugated long-TGT. These intermediate complexes were then incubated with biotinylated ssDNA binding protein (SSB, from *E. coli*) at a 1:1 molar ratio, making the final complex of btSSB:ssDNA TGT. The 4 pN tether was characterized using optical tweezers as described in Chowdhury *et al.*(*5*).

Cell culture and treatment.

In order to monitor Notch activation through the different tension tolerance TGTs, CHO-K1 cells containing a transgenic Notch reporter were utilized as shown previously in Wang *et al*. and Chowdhury *et al.*(*3*, *5*). The cells were incubated on the ligand-ProG-TGT immobilized surface for 48 hours. H2B-YFP expression level resulting from Notch activation was monitored by a fluorescence microscope (Olympus, IX81, Olympus Inc.). The intensity of H2B-YFP in each cell was analyzed using ImageJ and the histogram was plotted based on the mean value of the H2B-YFP intensity per cell.

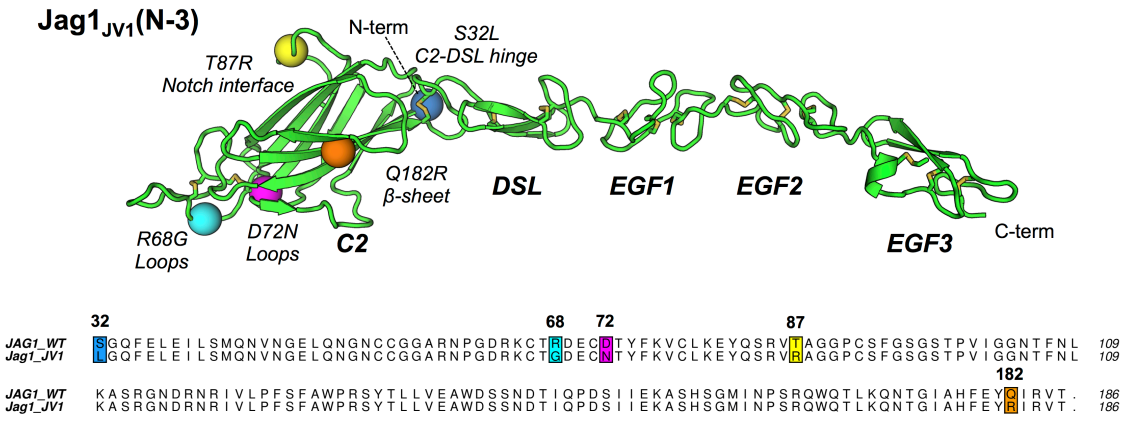

Figure S1. Affinity-enhancing mutations are located in the Jag1 C2 domain. The structure of $Jag1_{JV1}$(N-3) is depicted in cartoon representation. Affinity-enhancing mutations are indicated as colored spheres, and are highlighted on the corresponding sequence alignment of the WT Jag1 and $Jag1_{JV1}$ C2 domain regions.

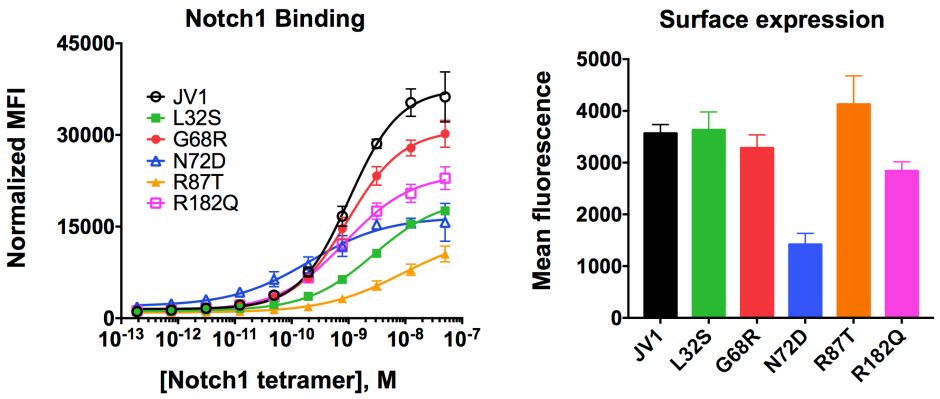

Variant	EC50	Expression level relative to JV1
JV1	1.03 nM	100%
L32S	2.79 nM	102%
G68R	0.98 nM	92%
N72D	0.20 nM	40%
R87T	8.76 nM	116%
R182Q	0.87 nM	80%

Figure S2. Binding of Notch1 to $Jag1_{JV1}$ constructs with affinity-enhancing mutations reverted to the wild type sequence. Yeast expressing $Jag1_{JV1}$(N-3), or expressing $Jag1_{JV1}$(N-3) with affinity-enhancing mutations reverted to the WT sequence, were stained with increasing concentrations of fluorescently labeled Notch1(8-12) tetramers. Curves were fitted to determine EC50 values. Surface expression of $Jag1_{JV1}$(N-3) and $Jag1_{JV1}$(N-3) mutants was monitored by staining with an antibody to the c-Myc epitope encoded by the displayed proteins.

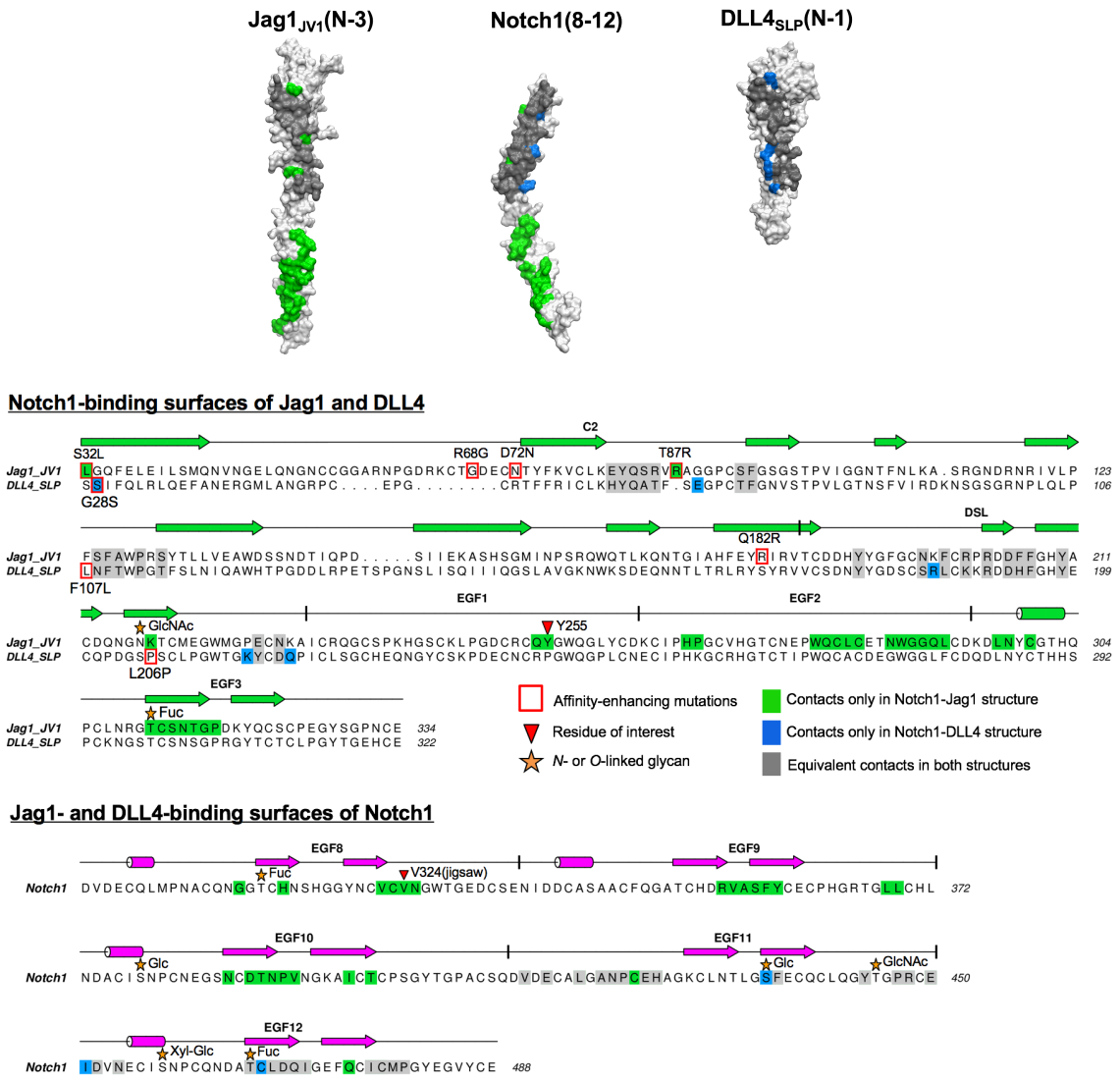

Figure S3. Structural comparison of Notch1-Jag1$_{JV1}$ and Notch1-DLL4$_{SLP}$ binding interfaces. Individual structures of Notch1(8-12) and Jag1$_{JV1}$(N-3) from the Notch1(8-12)-Jag1$_{JV1}$(N-3) complex, and the structure of DLL4$_{SLP}$(N-1) from the Notch1(11-13)-DLL4$_{SLP}$(N-1) complex (PDB ID: 4XL1), are depicted in surface representation(*20*). Grey residues of Jag1$_{JV1}$, DLL4$_{SLP}$ and Notch1 indicate that the analogous amino acid contributes to the binding interface in both structures. Green residues interact only in the Notch1(8-12)-Jag1$_{JV1}$(N-3) structure, and blue residues interact only in the Notch1(11-13)-DLL4$_{SLP}$(N-1) structure(*20*). The corresponding interface residues are color-coded accordingly on the sequence alignment. Glycans visible in the electron density maps, affinity-enhancing mutations, and residues discussed in the text and are also indicated on the alignment.

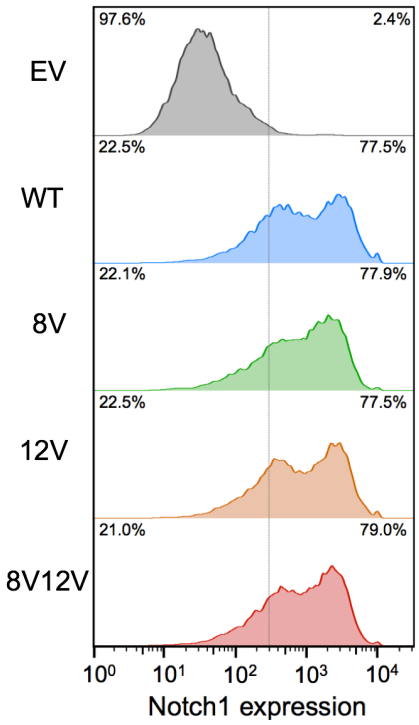

Figure S4. Surface expression of Notch1 and Notch1 mutants lacking O-fucose modifications. HEK293T cells expressing Notch1, and HEK293 cells expressing Notch1 proteins lacking interface *O*-fucose modifications in EGF8 (8V: Notch1 T311V), EGF12 (Notch1 T466V) or EGF8/EGF12 (8V12V: Notch1 T311V/T466V) were stained with an antibody to the ECD of Notch1. Surface expression was analyzed by flow cytometry. All mutations of *O*-fucose-modified threonines were to valines.

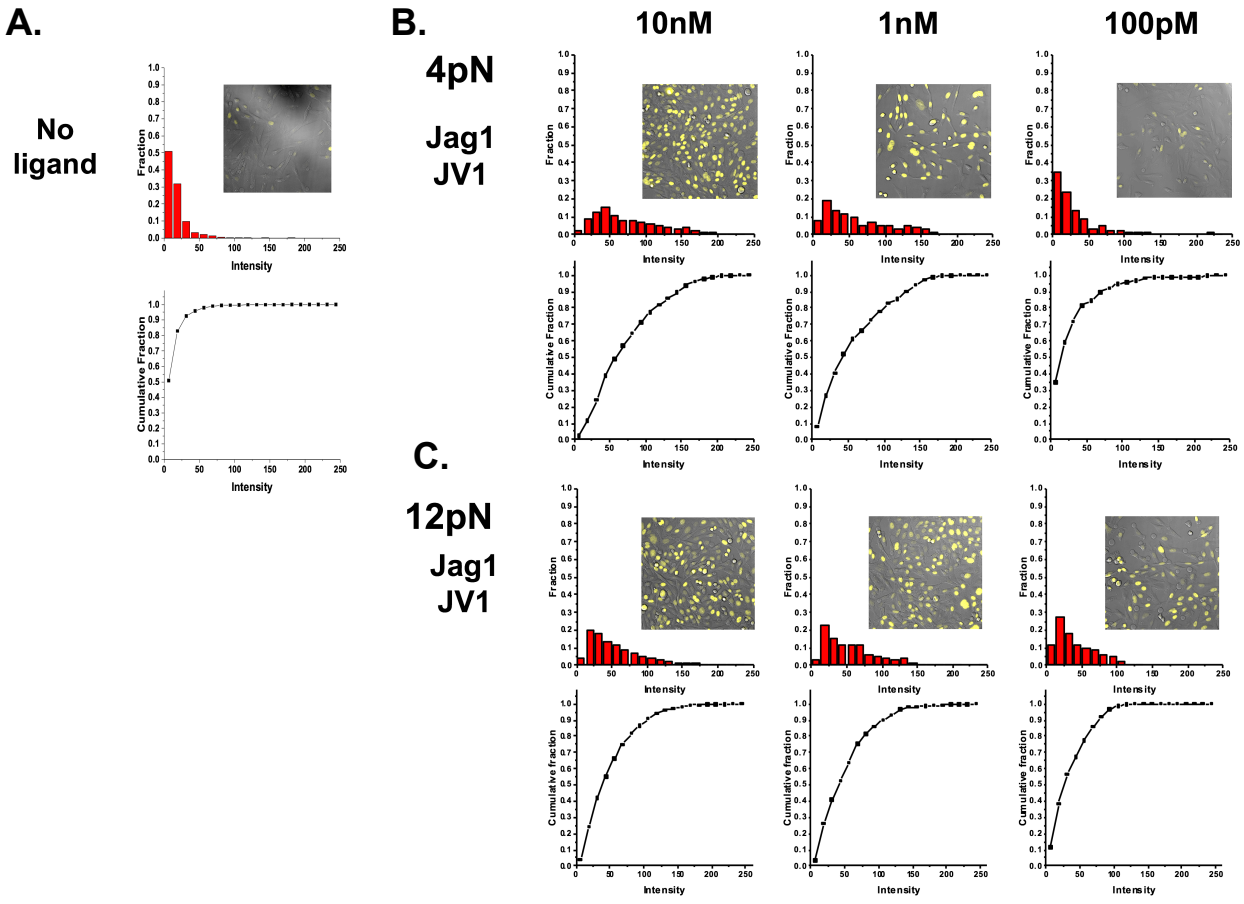

Figure S5. Notch activation is concentration dependent in TGT assays. Notch activation was monitored by H2B-YFP expression in transgenic CHO-K1 cells. $Jag1_{JV1}$(N-3) was incubated on the TGT surface at three different concentrations (10 nM, 1 nM, and 100 pM). Note that the 10 nM incubation concentration was used for the data presented in Figure 3. Each panel shows an example composite image of micrographs of adhered cells and YTF fluorescence, a YFP intensity histogram, and a cumulative fraction curve showing the fraction of cells with YFP intensity up to a certain level. (A) Negative control indicating that most cells were not activated without ligand TGT. (B) Notch activation on 4 pN $Jag1_{JV1}$-TGT surfaces using three different incubation concentrations. $Jag1_{JV1}$ strongly activated Notch with 10 nM and 1 nM incubation concentrations, but only weakly with a 100 pM incubation concentration. (C) Notch activation on 12 pN $Jag1_{JV1}$-TGT surfaces. Cells showed Notch activation in all tested conditions. We can conclude that lowering the frequency of attempts to activate Notch mechanically by lowering the ligand density reduces Notch signaling activation, and that we can compensate for this effect by increasing the mechanical strength of the tethers.

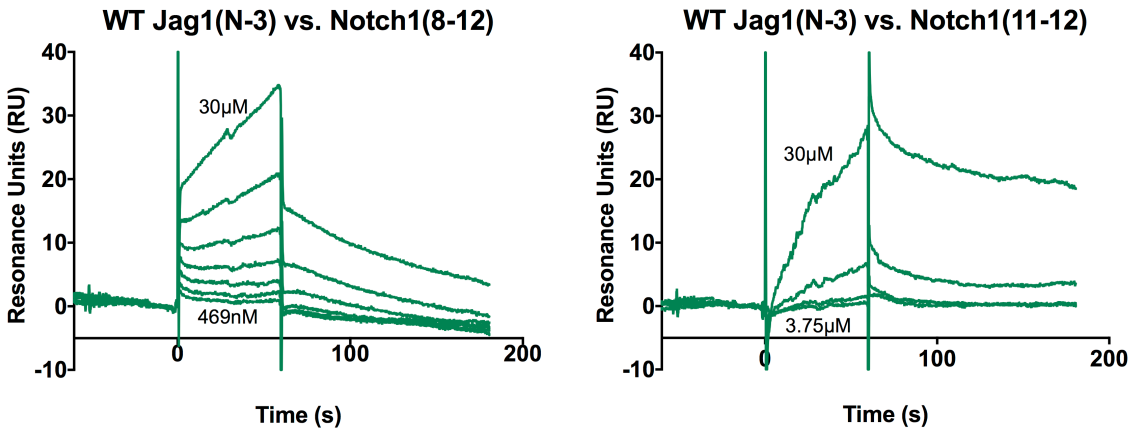

Figure S6. Binding of WT Jag1(N-3) to Notch1(8-12) and Notch1(11-12) observed by SPR. Various concentrations of Jag1(N-3) were injected over a sensor chip containing immobilized Notch1(8-12) or Notch1(11-12) (starting concentration 30 μM, decreasing by 2-fold dilutions). The highest and lowest concentrations are indicated on the sensograms. Binding levels of WT Jag1(N-3) to Notch1(8-12) and Notch1(11-12) were insufficient to allow for reliable determination of K_d values.

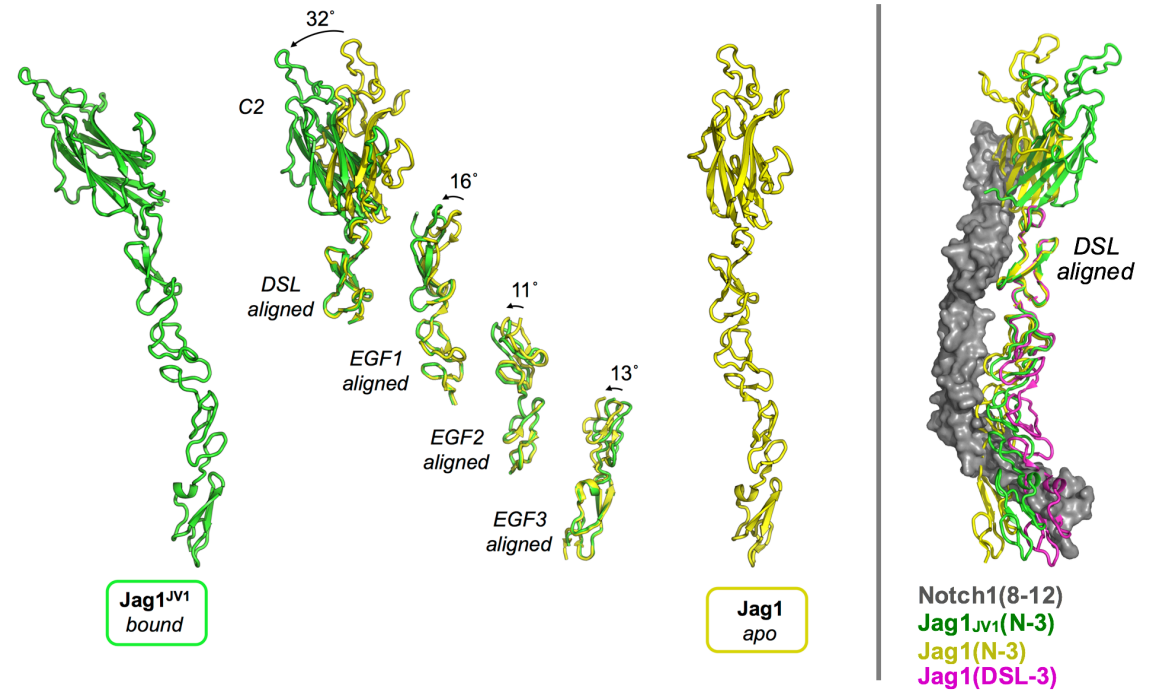

Figure S7. Jag1 inter-domain hinge motions. The structure of $Jag1_{JV1}$(N-3) from the Notch1(8-12)-$Jag1_{JV1}$(N-3) complex (green), and the previously reported structure of "apo" Jag1(N-3) (yellow, PDB ID: 4CC0), are depicted in cartoon representation(*17*). Domains from each structure were aligned individually and the rotation angles between each pair are indicated (left panel). The DSL domains of $Jag1_{JV1}$(N-3) in complex with Notch1(8-12) (shown as grey surface), apo Jag1(N-3), and Jag1(DSL-3) (magenta, PDB ID: 2VJ2) were aligned to highlight variability in the relative orientations of EGF domains 1 through 3 (right panel)(*10*). Note that EGF domains 1 through 3 of both Jag1(DSL-3) and Jag1(N-3) are predicted to clash with Notch1(8-12) from the complex structure.

Table 1. Data collection and refinement statistics for Notch1(8-12)-Jag1$_{JV1}$(N-3) complex

Data Collection	
Space group	$I2_12_12_1$
Cell dimensions	
a, b, c (Å)	68.5, 128.0, 154.3
α, β, γ (°)	90.0, 90.0, 90.0
Resolution (Å) (high-resolution shell)	44.7-2.5 (2.66-2.50)
R_{merge} (%)	9.1 (>100)
R_{pim} (%)	4.1 (60.8)
Redundancy	7.4 (7.4)
I/σ	18.3 (1.3)
Completeness (%)	99.2 (93.3)
CC1/2	0.734
Unique reflections	23569 (2192)
Refinement	
Resolution (Å) (high-resolution shell)	44.7-2.50 (2.62-2.50)
R_{work} reflections	23543 (2177)
R_{free} reflections	1178 (108)
R_{work}	21.9 (33.2)
R_{free}	26.3 (39.1)
Number of atoms	4033
Protein	3780
Ligand/ion	115
Water	138
Wilson B-factor (Å^2)	62
Average B-factor (Å^2)	94
Protein	95
Ligands	104
Solvent	78
R.m.s. deviations	
Bond lengths (Å)	0.007
Bond angles (°)	0.860
Ramachandran (%) (favored/allowed/outliers)	96.6/3.4/0.0
Molprobity clash score	8.2
TLS groups	13

Table 2. Comparison of polar contacts in Notch-ligand complex structures.

Notch1(8-12)-Jag1$_{JV1}$(N-3) complex

Notch1 aa[atom]	Distance	Jag1 aa[atom]
Hydrogen bonds		
FUC 311[O3]	3.33	ASN 298[ND2]
CYS 323[O]	3.03	ASN 314[ND2]
ASN 325[N]	2.66	LEU 297[O]
ASN 325[ND2]	3.03	ASN 314[O]
ASN 325[ND2]	2.94	THR 315[O]
ALA 355[O]	2.88	GLY 290[N]
SER 356[OG]	3.55	GLN 291[N]
SER 356[OG]	2.78	GLY 290[N]
THR 389[O]	3.88	TRP 280[NE1]
ASN 421[O]	2.94	ARG 203[NH2]
PRO 422[O]	3.47	ARG 203[NH1]
GLU 424[OE2]	3.85	TYR 210[OH]
HIS 425[NE2]	3.22	TYR 191[OH]
FUC 466[O4]	2.70	TYR 65[O]
ASP 469[O]	2.92	ALA 127[N]
Salt bridges		
GLU 424[OE2]	3.64	ARG 203[NH1]

Notch1(11-13)-DLL4$_{SLP}$(N-1) complex

Notch1 aa[atom]	Distance	DLL4 aa[atom]
Hydrogen bonds		
ASN 421[O]	3.65	ARG 191[NH1]
HIS 425[NE2]	3.28	TYR 179[OH]
BGC 435[O6]	2.64	ASP 218[OD2]
ARG 448[N]	3.65	TYR 216[OH]
ARG 448[NH1]	3.04	PHE 195[O]
GLU 450[O]	2.86	LEU 187[N]
GLU 450[OE2]	2.65	TYR 216[OH]
ASP 452[N]	2.89	SER 185[O]
FUC 466[O4]	2.70	TYR 65[O]
ASP 469[O]	3.00	THR 110[N]
ASP 469[O]	3.76	THR 110[OG1]
ASP 469[OD2]	2.94	THR 110[OG1]
ASP 452[N]	2.89	SER 185[O]
Salt bridges		
ARG 448[NH2]	3.45	ASP 218[OD2]

REFERENCES:

1. A. L. Parks, K. M. Klueg, J. R. Stout, M. A. Muskavitch, Ligand endocytosis drives receptor dissociation and activation in the Notch pathway. *Dev. Camb. Engl.* **127**, 1373–1385 (2000).
2. G. Chapman *et al.*, Notch1 endocytosis is induced by ligand and is required for signal transduction. *Biochim. Biophys. Acta*. **1863**, 166–177 (2016).
3. X. Wang, T. Ha, Defining Single Molecular Forces Required to Activate Integrin and Notch Signaling. *Science*. **340**, 991–994 (2013).
4. W. R. Gordon *et al.*, Mechanical Allostery: Evidence for a Force Requirement in the Proteolytic Activation of Notch. *Dev. Cell*. **33**, 729–736 (2015).
5. F. Chowdhury *et al.*, Defining Single Molecular Forces Required for Notch Activation Using Nano Yoyo. *Nano Lett.* **16**, 3892–3897 (2016).
6. W. R. Gordon *et al.*, Structural basis for autoinhibition of Notch. *Nat. Struct. Mol. Biol.* **14**, 295–300 (2007).
7. B. De Strooper *et al.*, A presenilin-1-dependent gamma-secretase-like protease mediates release of Notch intracellular domain. *Nature*. **398**, 518–522 (1999).
8. G. Struhl, I. Greenwald, Presenilin is required for activity and nuclear access of Notch in Drosophila. *Nature*. **398**, 522–525 (1999).
9. C. Brou *et al.*, A novel proteolytic cleavage involved in Notch signaling: the role of the disintegrin-metalloprotease TACE. *Mol. Cell*. **5**, 207–216 (2000).
10. J. Cordle *et al.*, A conserved face of the Jagged/Serrate DSL domain is involved in Notch trans-activation and cis-inhibition. *Nat. Struct. Mol. Biol.* **15**, 849–857 (2008).
11. P. C. Weisshuhn *et al.*, Non-Linear and Flexible Regions of the Human Notch1 Extracellular Domain Revealed by High-Resolution Structural Studies. *Struct. Lond. Engl. 1993*. **24**, 555–566 (2016).
12. C. Hicks *et al.*, Fringe differentially modulates Jagged1 and Delta1 signalling through Notch1 and Notch2. *Nat. Cell Biol.* **2**, 515–520 (2000).
13. D. J. Moloney *et al.*, Mammalian Notch1 is modified with two unusual forms of O-linked glycosylation found on epidermal growth factor-like modules. *J. Biol. Chem.* **275**, 9604–9611 (2000).
14. T. Okajima, K. D. Irvine, Regulation of Notch Signaling by O-Linked Fucose. *Cell*. **111**, 893–904 (2002).
15. S. Shi, P. Stanley, Protein O-fucosyltransferase 1 is an essential component of Notch signaling pathways. *Proc. Natl. Acad. Sci.* **100**, 5234–5239 (2003).
16. S. Kakuda, R. S. Haltiwanger, Deciphering the Fringe-Mediated Notch Code: Identification of Activating and Inhibiting Sites Allowing Discrimination between Ligands. *Dev. Cell* (2016), doi:10.1016/j.devcel.2016.12.013.
17. C. R. Chillakuri *et al.*, Structural analysis uncovers lipid-binding properties of Notch ligands. *Cell Rep.* **5**, 861–867 (2013).
18. N. J. Kershaw *et al.*, Notch ligand delta-like1: X-ray crystal structure and binding affinity. *Biochem. J.* **468**, 159–166 (2015).
19. I. Rebay *et al.*, Specific EGF repeats of Notch mediate interactions with Delta and Serrate: implications for Notch as a multifunctional receptor. *Cell*. **67**, 687–699 (1991).

20. V. C. Luca *et al.*, Structural biology. Structural basis for Notch1 engagement of Delta-like 4. *Science*. **347**, 847–853 (2015).
21. S. Yamamoto *et al.*, A mutation in EGF repeat-8 of Notch discriminates between Serrate/Jagged and Delta family ligands. *Science*. **338**, 1229–1232 (2012).
22. M. B. Andrawes *et al.*, Intrinsic selectivity of Notch 1 for Delta-like 4 over Delta-like 1. *J. Biol. Chem.* **288**, 25477–25489 (2013).
23. B. T. Marshall *et al.*, Direct observation of catch bonds involving cell-adhesion molecules. *Nature*. **423**, 190–193 (2003).
24. R. Rampal, J. F. Arboleda-Velasquez, A. Nita-Lazar, K. S. Kosik, R. S. Haltiwanger, Highly conserved O-fucose sites have distinct effects on Notch1 function. *J. Biol. Chem.* **280**, 32133–32140 (2005).
25. P. Taylor *et al.*, Fringe-mediated extension of O-linked fucose in the ligand-binding region of Notch1 increases binding to mammalian Notch ligands. *Proc. Natl. Acad. Sci. U. S. A.* **111**, 7290–7295 (2014).
26. A. Xu, L. Lei, K. D. Irvine, Regions of Drosophila Notch That Contribute to Ligand Binding and the Modulatory Influence of Fringe. *J. Biol. Chem.* **280**, 30158–30165 (2005).
27. W. Chen, J. Lou, C. Zhu, Forcing switch from short- to intermediate- and long-lived states of the alphaA domain generates LFA-1/ICAM-1 catch bonds. *J. Biol. Chem.* **285**, 35967–35978 (2010).
28. W. Thomas, For catch bonds, it all hinges on the interdomain region. *J. Cell Biol.* **174**, 911–913 (2006).
29. S. Chakrabarti, M. Hinczewski, D. Thirumalai, Plasticity of hydrogen bond networks regulates mechanochemistry of cell adhesion complexes. *Proc. Natl. Acad. Sci.* **111**, 9048–9053 (2014).
30. D. Sprinzak *et al.*, Cis-interactions between Notch and Delta generate mutually exclusive signalling states. *Nature*. **465**, 86–90 (2010).
31. G. Chao *et al.*, Isolating and engineering human antibodies using yeast surface display. *Nat. Protoc.* **1**, 755–768 (2006).
32. T. S. Walter *et al.*, Lysine methylation as a routine rescue strategy for protein crystallization. *Struct. Lond. Engl. 1993*. **14**, 1617–1622 (2006).
33. W. Minor, Z. Otwinowski, Processing of X-ray diffraction data collected in oscillation mode. *Methods Enzymol.* **276**, 307–326 (1997).
34. L. A. Kelley, M. J. E. Sternberg, Protein structure prediction on the Web: a case study using the Phyre server. *Nat. Protoc.* **4**, 363–371 (2009).
35. P. D. Adams *et al.*, PHENIX: a comprehensive Python-based system for macromolecular structure solution. *Acta Crystallogr. D Biol. Crystallogr.* **66**, 213–221 (2010).
36. A. J. McCoy *et al.*, Phaser crystallographic software. *J. Appl. Crystallogr.* **40**, 658–674 (2007).
37. P. Emsley, K. Cowtan, Coot: model-building tools for molecular graphics. *Acta Crystallogr. D Biol. Crystallogr.* **60**, 2126–2132 (2004).
38. J. Painter, E. A. Merritt, Optimal description of a protein structure in terms of multiple groups undergoing TLS motion. *Acta Crystallogr. D Biol. Crystallogr.* **62**, 439–450 (2006).

39. J. Painter, E. A. Merritt, TLSMD web server for the generation of multi-group TLS models. *J. Appl. Crystallogr.* **39**, 109–111 (2006).
40. E. Krissinel, K. Henrick, Inference of macromolecular assemblies from crystalline state. *J. Mol. Biol.* **372**, 774–797 (2007).
41. *The PyMOL Molecular Graphics System, v1.5.0.5,* Schrödinger, LLC.
42. R. A. Lee, M. Razaz, S. Hayward, The DynDom Database of Protein Domain Motions. *Bioinformatics*. **19**, 1290–1291 (2003).
43. N. A. Rana *et al.*, O-glucose trisaccharide is present at high but variable stoichiometry at multiple sites on mouse Notch1. *J. Biol. Chem.* **286**, 31623–31637 (2011).
44. W. Chen, E. A. Evans, R. P. McEver, C. Zhu, Monitoring Receptor-Ligand Interactions between Surfaces by Thermal Fluctuations. *Biophys. J.* **94**, 694–701 (2008).
45. E. Evans, K. Ritchie, R. Merkel, Sensitive force technique to probe molecular adhesion and structural linkages at biological interfaces. *Biophys. J.* **68**, 2580–2587 (1995).
46. S. E. Chesla, P. Selvaraj, C. Zhu, Measuring two-dimensional receptor-ligand binding kinetics by micropipette. *Biophys. J.* **75**, 1553–1572 (1998).
47. X. Wang *et al.*, Constructing modular and universal single molecule tension sensor using protein G to study mechano-sensitive receptors. *Sci. Rep.* **6**, 21584 (2016).